Fast Fractal Stack: Fractal Analysis of Computed Tomography Scans of the Lung

Alceu Ferraz Costa, Joe Tekli, Agma Juci Machado Traina
Department of Computer Science
University of São Paulo
São Carlos, Brazil
{alceufc, joe.tekli, agma}@icmc.usp.br

ABSTRACT

This paper proposes a new feature extraction method: the Fast Fractal Stack, or FFS. The extraction algorithm consists in decomposing the input grayscale image into a stack of binary images from which the fractal dimension values are computed, resulting in a compact and highly descriptive set of features. We evaluated FFS for the task of classification of interstitial lung diseases in computed tomography (CT) scans, applied on a database of 248 CT images from 67 patients. The proposed approach performs well, improving the classification accuracy when compared to other feature extraction algorithms. Additionally, the FFS extraction algorithm is efficient, with a computational cost linear with respect to input image size.

Categories and Subject Descriptors

I.4.7 [**Image Processing and Computer Vision**]: Feature measurement—*feature representation*; J.3 [**Life and Medical Sciences**]: Medical Information Systems

General Terms

Algorithms, experimentation

Keywords

Feature extraction, Fractal analysis, Computer-aided diagnosis, Computed tomography, Interstitial lung diseases

1. INTRODUCTION

Computer aided diagnosis (CAD) of interstitial lung diseases (ILDs) is a major subject in high-resolution computed tomography (HRCT) [18, 13, 9, 16]. This can be attributed to the fast progress in computed tomography (CT) acquisition technology, and also to the fact that the interpretation of HRCT images of the chest from patients affected with ILDs is a challenging and time-consuming task even for experienced radiologists [5]. Additionally, a reliable CAD system could alleviate the radiologists' manual labor and avoid surgical lung biopsies.

The typical set-up of a CAD system consists in the extraction of relevant visual features in the form of feature vectors that are used as input to a classifier. Due to the infamous *semantic gap* problem [6], which corresponds to the difference between the physicians' image perception and the features automatically extracted from the image, a challenging aspect of the feature extraction task is to obtain a set of features (i.e. a feature vector) that is able to succinctly and efficiently represent the visual contents of medical images, supporting the specialist in the decision making process. A way to accomplish this goal would be to extract as many features as possible from the images, in order to describe most of their visual information. However, the use of a large number of features would result in a problem known as the *curse of dimensionality* [11], where the significance and informativeness of each feature decreases, making the classification process inaccurate and also time consuming.

Thus, it is important to identify and remove irrelevant and redundant attributes. Feature selection and feature transformation are two major techniques that can be used for this purpose. In attribute selection, a classification algorithm (or a given metric based on general characteristics of the data) is used to evaluate and select a subset of features from the original set of features. An example of an attribute selection method is the correlation-based feature selection (CFS) [7]. CFS uses the features' predictive performances and intercorrelations to find a good feature subset. In contrast, feature transformation methods take as input a set of features and use a transformation technique to create new features. Feature transformation methods such as the principal component analysis (PCA), are able to generate features that can be ordered based on their descriptive power. Therefore, it is possible to reduce dimensionality by discarding less descriptive features.

The disadvantage of feature selection and feature transformation is that they demand extra computational cost. As an alternative approach to deal with both problems, that is, the *semantic gap* and the *curse of dimensionality*, we propose a method based on fractal geometry, entitled Fast Fractal Stack (FFS), that extracts a compact and highly descriptive feature vector to describe grayscale images. FFS consists of two main steps: i) applying an adapted image partitioning technique (binary stack decomposition [3]) in order to transform the input image into a set of binary images, and then ii) computing, for each binary image, the fractal dimension corresponding to its regions' boundaries.

MMAR'11, November 29, 2011, Scottsdale, Arizona, USA.

Experiments performed with regions of interest (ROIs) of lung computed tomography (CT) show that the proposed method is able to classify different disease patterns with accuracy higher than 84% without using feature selection or feature transformation. Moreover, our proposed method is efficient, running in linear time with respect to the image size (number of pixels).

As for the classification phase, we make use of an SVM (Support Vector Machine) classifier, built on a polynomial kernel using the SMO (Sequential Minimal Optimization) algorithm [12]. We chose SVM due to its effectiveness and wide exploitation in medical image classification and related applications [4, 19]. The remainder of the paper is structured as follows. Section 2 discusses preliminary concepts and techniques. Section 3 describes the proposed feature extraction method. Results from the experiments are interpreted and discussed in section 4. Final conclusions are drawn in section 5. The symbols used throughout the paper are listed in Table 1.

Table 1: Table of symbols

Symbol	Definition
I	Grayscale image.
I_b	Binary image.
Δ	Border image.
n_l	Gray level range.
T	Set of thresholds used to generate the binary image stack.
n_t	Number of elements in T.
D	Fractal dimension.
E	Euclidean dimension.
D_0	Haussdorf fractal dimension.
ϵ	Box size in the box counting algorithm.
V_D	FFS Feature vector.

2. BACKGROUND AND TECHNIQUES

A grayscale image I can be modeled as a 2D function $I(x, y)$, where $I(x, y) \in \{0, 1, \cdots, n_l - 1\}$. $I(x, y)$ is called the grayscale value or intensity of the pixel at position (x, y). Prior to the feature vector extraction phase, we employ the binary stack decomposition technique [3] to partition the input grayscale image I by applying successive thresholding operations. The goal is to separate structures and objects of different gray level intensities into different binary images.

When an image $I(x, y)$ is thresholded by a value t, $t \in \{0, 1, \cdots, n_l - 1\}$, a corresponding binary image is obtained. That is:

$$I_b(x, y; t) = \begin{cases} 1 \text{ if } I(x, y) \geq t \\ 0, \text{ otherwise.} \end{cases} \quad (1)$$

where $I_b(x, y; t)$ denotes the binary image obtained with the threshold t. For a given original image, there are n_l potentially different binary images. We refer to this set of binary images as a binary image stack. To describe the boundary complexity of objects and structures that were segmented by binary stack decomposition we apply fractal analysis.

In Euclidean geometry, the dimension is a natural number, i.e., a point possesses a dimension equal to 0, a straight line has dimension 1, a plane has dimension 2, a solid possesses dimension 3, and so on. However, modern (19th century) mathematics developed by Hausdorff, Koch and Sierpinsk put forward Fractal Geometry, a geometric theory suggesting that shapes and objects may have fractional dimensions as a consequence of the self-similarity property. In the image analysis paradigm, fractal dimension measurements are used to estimate and quantify the complexity of the shape or texture of objects [14, 1].

Fractal geometry involves various approaches to define fractional dimensions, the most common of which is the Hausdorff's dimension. Considering an object that possesses an Euclidean dimension E, the Hausdorff's fractal dimension D_0 can be computed by the following expression:

$$D_0 = \lim_{\epsilon \to 0} \frac{\log N(\epsilon)}{\log \epsilon^{-1}} \quad (2)$$

where $N(\epsilon)$ is a counting of cubes of dimension E and length ϵ that fill the object.

If we consider an object represented by a binary image I_b, an approximation D for D_0 can be obtained through the box counting algorithm [15]. Without loss of generality, let us explain the algorithm for the 2D case. Initially, the image is divided into a grid composed of squares of size $\epsilon \times \epsilon$. The next step consists in counting the number $\bar{N}(\epsilon)$ of squares of size $\epsilon \times \epsilon$ that contains at least one pixel of the shape. By varying the value ϵ, it is possible to create a $\log \bar{N}(\epsilon)$ vs $\log \epsilon^{-1}$ curve. Finally, this curve is approximated by a straight line using a line fitting method (e.g. least squares fitting). The fractal dimension D corresponds to the slope of this line.

3. PROPOSED METHOD

The FFS that we propose is a feature extraction method consisting of two main steps: first we apply the binary stack decomposition to the input grayscale image, resulting in a set of binary images. Then, for each binary image, we compute the fractal dimension from its regions' boundaries.

The regions' boundaries of a binary image $I_b(x, y; t)$ are represented as a border image denoted by $\Delta(x, y; t)$ and computed as follows:

$$\Delta(x, y; t) = \begin{cases} 1 \text{ if } \exists (x', y') \in N_8[(x, y)] : \\ \quad I_b(x', y'; t) = 0 \ \wedge \\ \quad I_b(x, y; t) = 1, \\ 0, \text{ otherwise.} \end{cases} \quad (3)$$

where $N_8[(x, y)]$ is the set of pixels that are 8-connected to (x, y). $\Delta(x, y; t)$ takes the value 1 if the pixel at position (x, y) in the corresponding binary image $I_b(x, y; t)$ has the value 1 and having at least one neighboring pixel with value 0. Otherwise, $\Delta(x, y; t)$ takes the value 0. Hence, one can realize that the resulting borders are one-pixel wide.

The fractal dimension $D(t)$, where t indicates the threshold value used to obtain the border image $\Delta(x, y; t)$, is computed using the box counting algorithm described in section 2. The value $D(t)$ describes the boundary complexity of the objects that were segmented using the threshold t.

By changing the value t it is possible to generate a curve $D(t) \times t$. We use this curve as a feature vector to describe the boundary complexity of structures and objects segmented by

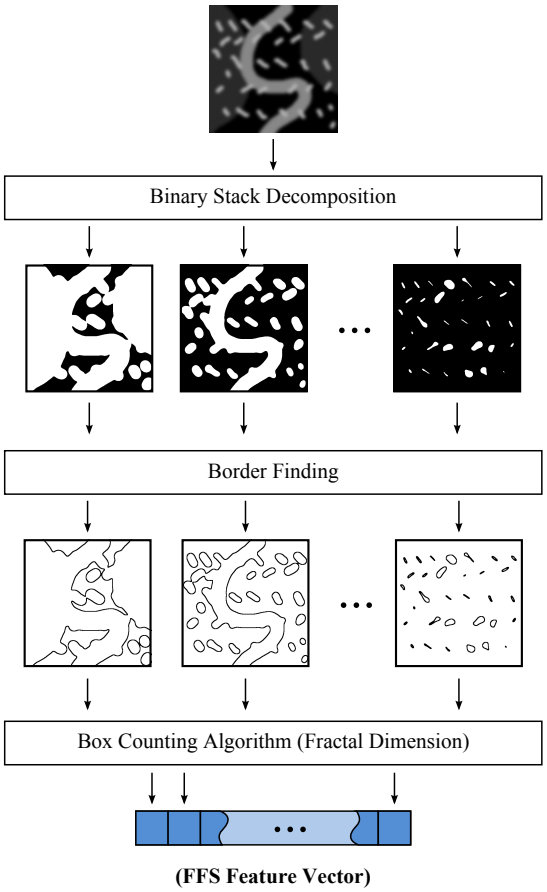

Figure 1: FFS extraction scheme taking as input an artificial grayscale image.

different threshold values. This procedure is illustrated in the diagram of figure 1.

There are two main reasons to use the curve $D(t) \times t$ instead of a single value $D(t)$ computed from a single threshold to describe an image. First, there is the non-trivial and domain dependent task of finding the correct threshold value that segments the structures and objects from the background. Second, for some images, a binary segmentation may be inadequate and, hence, a single threshold value may not produce a satisfactory result. For example, a single medical imaging exam may contain more than two different anatomical structures, each of which with different gray level ranges. This will be further exemplified in section 4, where we discuss the application of the proposed method for the specific task of lung tissue classification.

Algorithm 1 summarizes the steps of the FFS feature extraction process. Note that V_D denotes the resulting feature vector. In line 2, T is a set of all possible gray level values that an image I can take. The **Threshold** procedure in line 3 thresholds the image I by a gray level t as described in equation 1. The **FindBorders** procedure in line 4 corresponds to equation 3.

Note that the fractal dimension can be efficiently computed in linear time by the box counting algorithm proposed in [17]. Thus, the complexity of the FFS extraction algorithm is $O(N \cdot |T|)$, where N is the number of pixels in the grayscale image I, and $|T|$ is the number of different threshold values used to generate the binary image stack. As we will discuss in the next section, T is only a small subset of all possible threshold values. Therefore, the FFS extraction runs in linear time with respect to the image size.

Algorithm 1 Fast Fractal Stack (FFS).

Require: Grayscale image I.
Ensure: Feature vector V_D.
1: $i \leftarrow 0$
2: **for** $t \in T \subseteq \{0, 1, \cdots, n_l\}$ **do**
3: $I_b(x, y; t) \leftarrow$ **Threshold**$(I,\ t)$
4: $\Delta(x, y; t) \leftarrow$ **FindBorders**$(I_b(x, y; t))$
5: $D(t) \leftarrow$ **BoxCounting**$(\Delta(x, y; t))$
6: $V_D[i] \leftarrow D(t), \quad i \leftarrow i + 1$
7: **end for**
8: **return** V_D

3.1 FFS Feature Vector Dimensionality

The number of features extracted by the FFS algorithm corresponds to the number of different thresholds used to generate the binary image stack. That is, each binary image contributes with one value of $D(t)$ to the resulting feature vector. If all n_l possible threshold values are used, the resulting feature vector will be composed of n_l features. For example, if an image pixel can take 256 different gray level values, the maximum number of features extracted from this image will also be 256.

Intuitively, one may think that using all possible threshold values may result in better classification accuracy, because a large number of features will be generated, introducing more information into the classification process. However, this is not true for two main reasons. First, binary images obtained by contiguous thresholds tend to be very similar, resulting in highly correlated fractal dimension values that do not add useful information into the classification process. Second, as discussed in section 1, the classification performance degrades as the number of attributes increases, due to the curse of dimensionality.

To overcome both problems, we adopt the strategy of selecting a fixed number of equally spaced thresholds:

$$t_i = \left\lfloor \frac{n_l}{n_t + 1} \cdot i \right\rfloor, \quad i = 1, 2, \cdots, n_t \tag{4}$$

where n_t is the number of threshold values to be selected. In our experiments, we empirically set n_t equal to 8. Although simple, this strategy has shown to be effective in pratice (as we describe in section 4), obtaining results that were equivalent (and sometimes better) than choosing the thresholds by the supervised selection of attributes using Correlation-based Feature Selection (CFS) method. Additionally, the approach we adopt does not require any knowledge about the class distribution of the image set.

4. INTERSTITIAL LUNG DISEASE CLASSIFICATION

Considering a computed tomography (CT) image, the structures have their brightness measured in the image according to its ability to absorb the incident X-ray. The air, for example, is less dense than water, and therefore presents a

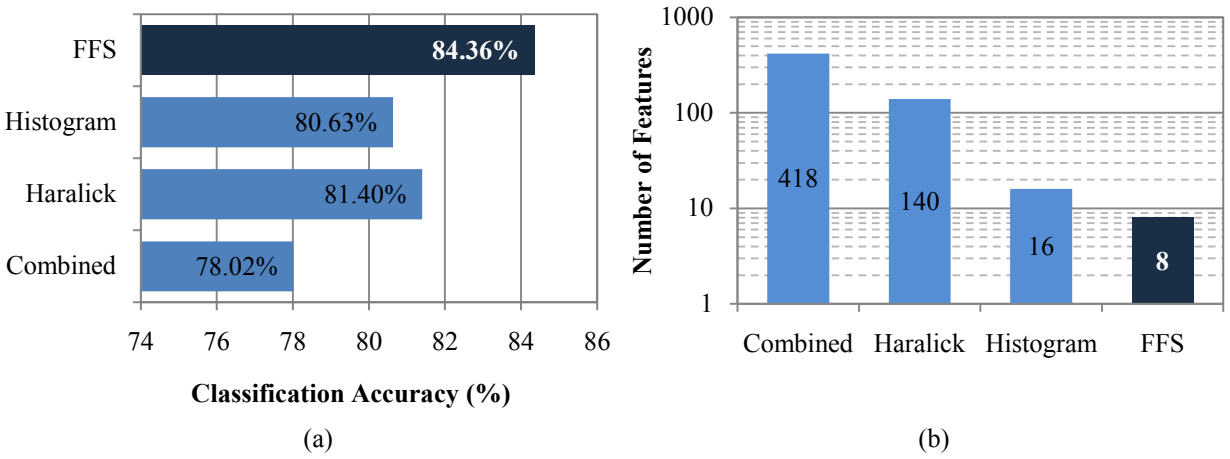

Figure 3: (a) Classification accuracy for the proposed FFS method, histogram, Haralick and combined feature vector without feature selection. (b) Feature vector size for each extraction method.

lower value of brightness in the image. Thus, it is possible to identify different tissues in a CT scan image depending on their attenuation coefficient.

We evaluate the FFS extraction method for the task of classifying interstitial lung diseases (ILDs). We use the FFS feature extraction algorithm to decompose a lung CT scan image into a binary image stack where each binary image corresponds to tissues of different attenuation coefficients. The border complexity measure of each binary image is then used to predict the occurrence of ILDs that are characterized by alterations in the healthy pulmonary tissue.

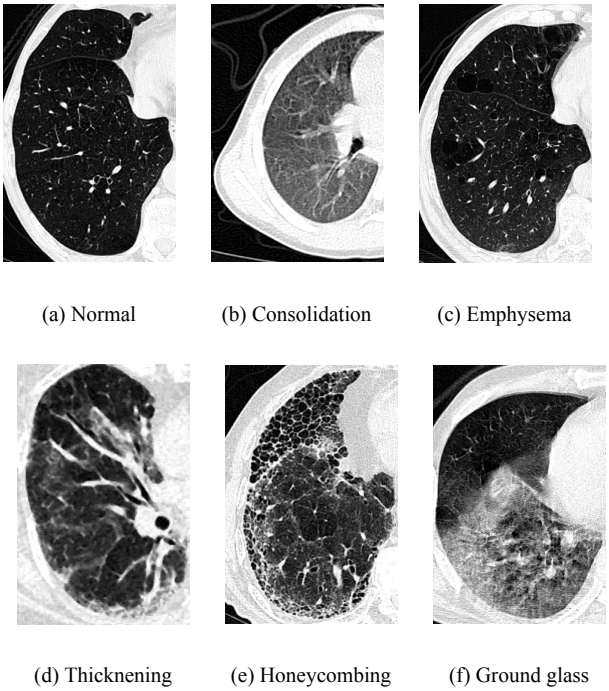

Figure 2: Examples of CT images with (a) normal slice and abnormal slices with (b) consolidation, (c) emphysema, (d) thicknening, (e) honeycombing, (f) ground glass.

To evaluate the proposed feature extraction method, clinical cases were selected from CT images from the Clinical Hospital at Ribeirão Preto of the University of São Paulo - Brazil based on normal cases and abnormal cases, reported in clinical exams from 2001 to 2006. Our image database included 248 CT images selected from 67 patients. The image size was 512×512 pixels and the slice thickness was 1mm. The bit-depth was 12 and was converted to 8 for the feature extraction process.

The preparation of the image base consisted in first segmenting the lungs from the background in each CT slice. Contiguous regions of interest (ROIs) with a matrix size of 64×64 pixels and an overlap of 16 pixels between two adjacent ROIs were selected over the segmented lung region.

Each ROI was classified by a specialist as normal or as an ILD pattern. The ILD patterns, shown at Figure 2, were the following: (i) emphysematous change, (ii) consolidation, (iii) interlobular septal thickening, (iv) honeycombing and (v) ground-glass opacities. Table 2 shows the class distributions for the ROIs selected from our CT image base.

Table 2: Class distribution for the ROIs selected from the CT image base.

Class	Number of ROIs
Consolidation	451
Emphysema	502
Thicknening	590
Honeycombing	530
Normal	590
Ground Glass	595

We used as baseline comparison traditional features, such as the gray level histogram and the Haralick descriptors, widely employed in many works [18, 2] that consider CT lung images. In order to perform histogram extraction, we re-quantized the CT ROIs to 16 gray levels, resulting in a feature vector with 16 features. As a measure of the ROIs' texture, we employed the Haralick descriptors [8] based on statistical moments obtained from the image co-occurrence matrix, resulting in a feature vector with 140 components.

Additionally, we combined the Haralick and histogram features with Zernike moments [10] and histogram statistics, creating a single feature vector with 418 components. We refer to this combined feature vector with the term "combined".

We applied an SVM classifier with a polynomial kernel using the SMO algorithm for comparing the FFS accuracy with the other extractors. The best SVM parameters were evaluated by 10-fold cross validation.

Figure 3(a) shows the classification accuracy obtained using each feature extraction method. The results were obtained by 10-fold cross validation with the SVM classifier with 10 repetitions. The FFS produced an average classification accuracy of 84.4%, outperforming the other extraction methods.

Additionally, as it is shown in figure 3(b), the FFS has the advantage of providing a feature vector with a smaller number of features when compared to the other extraction methods, what is meaningful regarding the curse of dimensionality. Figure 4 depicts the results obtained when applying Principal Component Analysis (PCA) and Correlation-based Feature Selection (CFS) to reduce the number of features of the Haralick, histogram and combined feature vectors to 8, which is the same number of features of the FFS feature vector. Figure 4(a) shows the gain and loss of classification accuracy after employing PCA and CFS. Results in Figure 4(b) show that FFS produced higher classification accuracy in comparison with the other methods. This indicates that the FFS provides a more compact and highly descriptive representation of ILD patterns.

We have also investigated the performance of the classification between normal ROIs and abnormal ROIs. ROIs classified as ILD patterns were considered positive cases and normal ROIs were considered negatives cases. By varying the SVM positive classification threshold value, receiver operating characteristics (ROC) curves were generated as plots of true positive rate (TPR) vs. false positive rate (FPR). Figure 5(a) shows ROC curves for the feature extraction methods. Since the top left corner ($\mathrm{TPR} = 1.0, \mathrm{FPR} = 0.0$) of the ROC space corresponds to the optimum classifier operation point, the Figure 5(b) zooms into the most interesting part of the curve. Results in Figure 5(b) show that FFS resulted in superior classification quality, in comparison with Haralick, histogram and combined feature vectors.

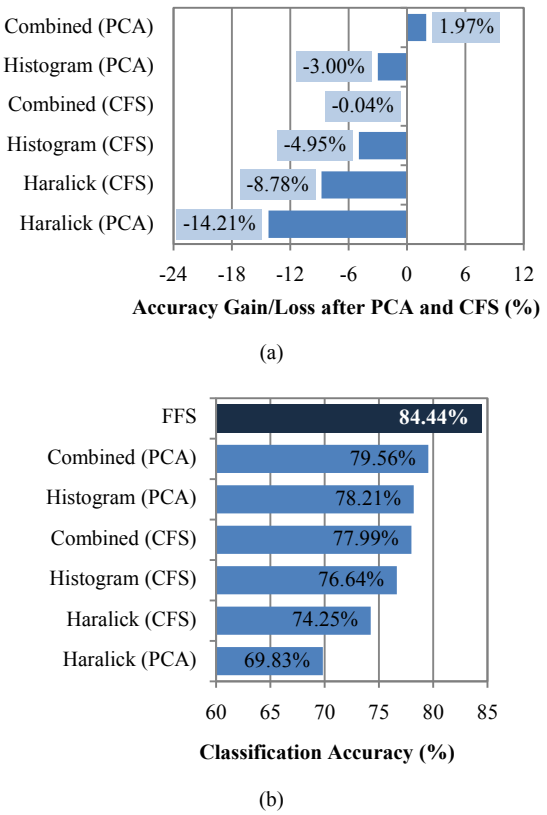

Figure 4: (a) Gain and loss of classification accuracy after employing PCA and CFS to the histogram, Haralick and combined feature vectors. (b) Comparison of the classification accuracy with the proposed FFS method.

5. CONCLUSIONS

In this paper we proposed a new feature extraction method called Fast Fractal Stack (FFS). The FFS employs fractal analysis to measure the border complexity of structures and objects of grayscale images and provides a compact and highly descriptive feature vector.

We have evaluated the proposed descriptor for classifying interstitial lung diseases (ILDs) from lung CT scans. Experimental results have highlighted the effectiveness of the FFS method in classifying normal lungs with respect to five different types of interstitial lung disease patterns.

Additionally, FFS provides an efficient extraction algorithm. While most feature extraction methods are at least quadratic, the computational cost of the extraction algorithm proposed in this paper is linear in the image size (number of pixels), based on the linear time algorithm to compute the fractal dimension. Therefore, FFS is a promising solution for content-based image retrieval systems supporting interactive decision making processes.

Considering the compactness of the resulting vector representation and the efficiency of the extraction algorithm, we are currently investigating the extension and exploitation of FFS in applications which specifically require low-dimensional features, such as the indexing and retrieval of images.

6. ACKNOWLEDGEMENTS

This research has been supported by FAPESP (São Paulo State Research Foundation), CNPq (Brazilian National Research Council), CAPES (Brazilian Coordination for Improvement of Higher Level Personnel) and Microsoft Research.

7. REFERENCES

[1] A. G. R. Balan, A. J. M. Traina, C. Traina Jr., and P. M. A. Marques. Fractal analysis of image textures for indexing and retrieval by content. In *18th IEEE Symposium on Computer-Based Medical Systems, 2005. Proceedings*, pages 581–586, 2005.

[2] P. H. Bugatti, M. Ponciano-Silva, A. J. M. Traina, C. Traina Jr., and P. M. A. Marques. Content-based retrieval of medical images: From context to

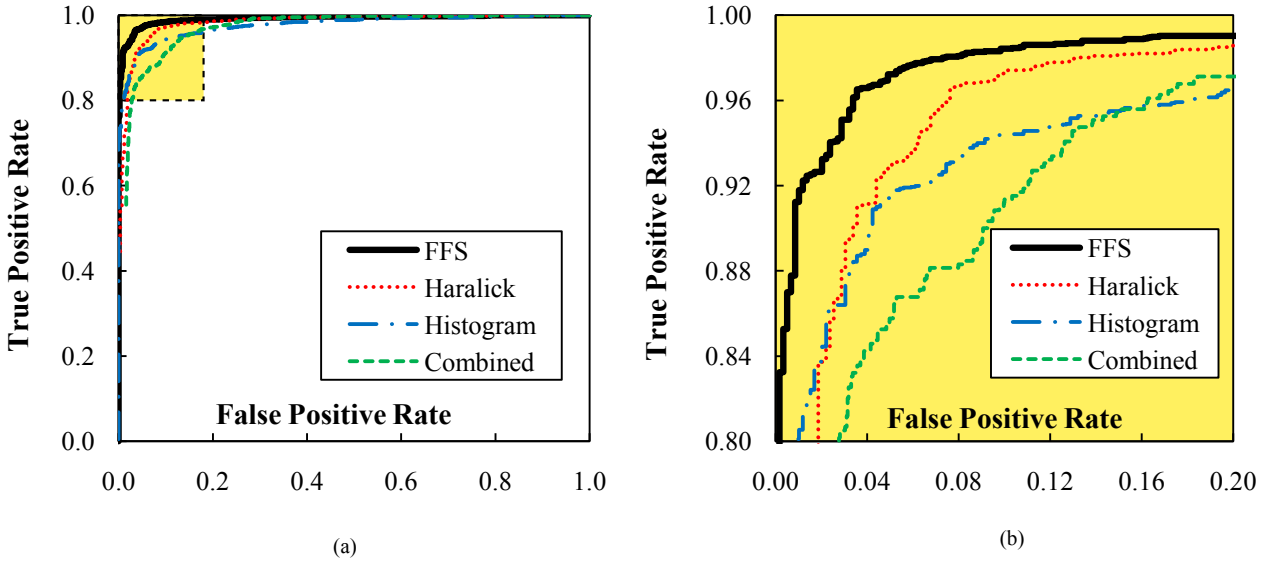

Figure 5: (a) ROC curve for the detection of interstitial lung diseases in the selected lung CT ROIs. (b) Zoom of the curve (a) into the optimum classifier operation point of the ROC space.

perception. In *22nd IEEE International Symposium on Computer-Based Medical Systems*, pages 1–8, Albuquerque, USA, Aug. 2009. IEEE.

[3] Y. Q. Chen and M. S. Nixon. Statistical geometrical features for texture classification. *Pattern Recognition*, 28(4):537–552, 1995.

[4] A. Depeursinge, J. Iavindrasana, A. Hidki, G. Cohen, A. Geissbuhler, A. Platon, P. Poletti, and H. Muller. A classification framework for lung tissue categorization. In *SPIE Medical Imaging*, volume 41, pages 69190C–69190C–12. SPIE, 2008.

[5] A. Depeursinge, D. Racoceanu, J. Iavindrasana, G. Cohen, A. Platon, P. A. Poletti, and H. Müller. Fusing visual and clinical information for lung tissue classification in high-resolution computed tomography. *Artificial intelligence in medicine*, 50:13–21, May 2010.

[6] T. M. Deserno, S. Antani, and R. Long. Ontology of gaps in content-based image retrieval. *Journal of digital imaging: the official journal of the Society for Computer Applications in Radiology*, 22(2):202–15, Apr. 2009.

[7] M. A. Hall. Correlation-based feature selection for discrete and numeric class machine learning. In *17th International Conference on Machine Learning*, pages 359–366, Stanford, CA, 2000.

[8] R. M. Haralick. Statistical and structural approaches to texture. In *Proceedings of the IEEE*, volume 67, pages 786–804, 1979.

[9] M. B. Huber, M. Nagarajan, G. Leinsinger, L. A. Ray, and A. Wismuller. Classification of interstitial lung disease patterns with topological texture features. In *Proceedings SPIE Medical Imaging 2010*, volume 7624, pages 2–9, 2010.

[10] A. Khotanzad and Y. H. Hong. Invariant image recognition by Zernike moments. *IEEE Transactions on Pattern Analysis and Machine Intelligence*, 12(5):489–497, May 1990.

[11] H. P. Kriegel, P. Kröger, and A. Zimek. Clustering high-dimensional data. *ACM Transactions on Knowledge Discovery from Data*, 3(1):1–58, Mar. 2009.

[12] J. Platt. *Fast training of support vector machines using sequential minimal optimization*, chapter 12, pages 185–208. MIT Press, Cambridge, MA, USA, 1999.

[13] M. Ponciano-Silva, A. J. M. Traina, P. M. A. Marques, J. C. Felipe, and C. Traina Jr. Including the perceptual parameter to tune the retrieval ability of pulmonary CBIR systems. In *22nd IEEE International Symposium on Computer-Based Medical Systems*, pages 1–8, Albuquerque, USA, Aug. 2009. IEEE.

[14] R. M. Rangayyan. Fractal analysis of contours of breast masses in mammograms. *Journal of Digital Imaging*, 20(3):223–37, Sept. 2007.

[15] M. Schroeder. *Fractals, Chaos, Power Laws: Minutes from an Infinite Paradis*. W. H. Freeman, New York, NY, USA, 1992.

[16] I. Sluimer, A. Schilham, M. Prokop, and B. van Ginneken. Computer analysis of computed tomography scans of the lung: a survey. *Medical Imaging, IEEE Transactions on*, 25(4):385–405, Apr. 2006.

[17] C. Traina Jr., A. J. M. Traina, L. Wu, and C. Faloutsos. Fast feature selection using fractal dimension. In *Proc. XV Brazilian Symposium on Databases (SBBD)*, pages 158–171, 2000.

[18] Y. Uchiyama, S. Katsuragawa, H. Abe, J. Shiraishi, F. Li, Q. Li, C. T. Zhang, K. Suzuki, and K. Doi. Quantitative computerized analysis of diffuse lung disease in high-resolution computed tomography. *Medical Physics*, 30(9):2440, 2003.

[19] D. Unay, O. Soldea, S. Ozogur-Akyuz, M. Cetin, and A. Ercil. Automated X-Ray Image Annotation. *Multilingual Information Access Evaluation II. Multimedia Experiments*, pages 247–254, 2011.